Microscopic analysis of the crystal field strength and lowest charge transfer energies in the elpasolite crystals Cs_2NaYX_6 (X=F, Cl, Br) doped with Cr^{3+}

M. G. Brik* and K. Ogasawara

Department of Chemistry and Open Research Center for Coordination Molecule-based Devices, School of Science and Technology, Kwansei Gakuin University, 2-1 Gakuen, Sanda, Hyogo 669-1337, Japan

(Received 16 April 2006; revised manuscript received 25 May 2006; published 7 July 2006)

Detailed microscopic study of the crystal field strength $10Dq$ and lowest charge transfer (CT) energies for different interionic distances in $Cs_2NaYX_6:Cr^{3+}$ (X=F, Cl, Br) crystals is performed in the present paper. The method used in the calculations is the first-principles fully relativistic discrete variational multielectron (DVME) method [K. Ogasawara *et al.*, Phys. Rev. B **64**, 115413 (2001)] based on solving Dirac equations with the local density approximation. From the results of performed calculations, the functions describing the dependencies of $10Dq$ and lowest CT energy on the metal-ligand distance R were obtained without introducing any fitting or semiempirical parameters. It was shown that $10Dq$ depends on R as $1/R^n$, with n=4.4634, 4.3742, and 4.3532 for $Cs_2NaYF_6:Cr^{3+}$, $Cs_2NaYCl_6:Cr^{3+}$, and $Cs_2NaYBr_6:Cr^{3+}$, respectively. The lowest CT energies E(CT) are linear functions of R and decrease with increasing R with $dE(\mathrm{CT})/dR$=−953 cm^{-1}/pm, −621 cm^{-1}/pm, and −520 cm^{-1}/pm for $Cs_2NaYF_6:Cr^{3+}$, $Cs_2NaYCl_6:Cr^{3+}$, and $Cs_2NaYBr_6:Cr^{3+}$, respectively. Using these results, the constants of the electron-vibronic interaction, Huang-Rhys parameters, Stokes shifts, and Gruneisen constants for the a_{1g} normal mode in all considered hosts were calculated. The obtained results are in good agreement with the experimental data and can be readily applied for analysis of the optical spectra and electron-vibronic interaction of the $[CrX_6]^{3-}$ (X=F, Cl, Br) units in other hosts.

DOI: 10.1103/PhysRevB.74.045105 PACS number(s): 78.20.Bh, 71.70.Ch, 71.70.Ej

I. INTRODUCTION

As is well known from crystal field theory, if any impurity ion with an unfilled electron shell is placed into a crystalline or glass host matrix, its energy levels are split due to the action of the crystal (ligand) field.[1–4] The splitting pattern is determined by the nature of an impurity ion and its nearest surroundings [in what follows this group of ions will be referred to as an "impurity center" (IC)], geometrical arrangement of the ligands (in other words, symmetry of IC), chemical bond lengths, etc. In the case of ions with a $3d$ open electron shell in a cubic crystal field this splitting is quantitatively described by so called cubic crystal field strength $10Dq$, which is equal to the energy separation between the antibonding e_g and t_{2g} orbitals of the central ion[1–4] (where e_g and t_{2g}indicate the symmetry properties of the wave functions of the split states transforming in accordance with corresponding irreducible representations of the O_h group). It was shown in the framework of the simplest point charge model of the crystal field[1] that $10Dq$ depends on the interionic separation R as $1/R^n$, n=5. However, the value of $10Dq$ predicted by this model is several times smaller than the experimental values,[5,6] and this is a clear indication that n deviates from 5. More elaborated models based on the molecular orbital calculations lead to n value in the 3.5–7.3 range.[7–9] It is highly desirable to know exactly how $10Dq$ depends on the distance between impurity ion and ligands, since such knowledge can help in getting valuable information about essential electronic properties of an IC, such as constants of electron-vibronic interaction (EVI), energetic Stokes shifts, Huang-Rhys parameters, compressibility, and Grüneisen parameters.[6–15] Therefore, a thorough microscopic analysis of the $10Dq(R)$ dependence for a number of impurity ions in various hosts is an important problem, and it is very attractive to tackle it by the first-principles methods in a systematic and consistent way to get a better insight into the microscopic structure of an IC. As earlier examples of such an analysis, we mention that detailed *ab initio* studies of $3d$ orbitals splitting for Cr^{3+} in fluorides,[6] Cr^{4+} in oxides,[9] microscopic treatment of the $S(a_{1g})$ Huang-Rhys factor,[7] optical spectra and pressure effects for V^{2+} and Cr^{3+} in elpasolites Cs_2NaYCl_6 and Cs_2NaYBr_6 (Refs. 11 and 16), and for Mn^{2+} in $KZnF_3$ (Ref. 17) were reported.

In the present paper we report on a systematic and consistent *ab initio* analysis of the dependence of the crystal field strength parameter $10Dq$ and lowest charge transfer (CT) energies on the distance between Cr^{3+} ion and ligands. The calculations were performed for three isostructural crystals from the elpasolite family, Cs_2NaYF_6, Cs_2NaYCl_6, and Cs_2NaYBr_6. We obtain the functional dependencies of both quantities on the distance, and use them for an estimation of the EVI constants, Huang-Rhys factors, bulk modulus, and Grüneisen parameters. The results obtained in the present study can be applied to IC formed by Cr^{3+} and halogen ions in other matrices as well.

The choice of the elpasolite crystals as the object of the present study was determined by the high symmetry (O_h) of the Cr^{3+} position. Besides, these materials have been the subject of many extensive experimental and theoretical studies[11,16,18–30] which results in a considerable amount of reliable information on their optical spectra and normal vibration frequencies.

The paper is organized as follows: in the next section we briefly describe the main ideas underlying the calculation method. Then we proceed with a short summary of crystal structure data for the considered materials, present the obtained results, and after a discussion conclude the paper with a brief summary.

II. METHOD OF CALCULATIONS

The method employed in the present calculations is the fully relativistic discrete variational multielectron (DVME) method developed by Ogasawara *et al.*[31] This is a configuration-interaction (CI) calculation program, which makes use of the four-component fully relativistic molecular spinors obtained by the discrete-variational Dirac-Slater (DV-DS) cluster calculations.[32] The DVME method is based on the numerical solution of the many-electron Dirac equation, and its main advantages are as follows: (1) the first-principles method without any phenomenological parameters (this is especially important for the development of new materials, prediction of their expected properties, and analysis of the common trends between similar compounds); (2) a very wide area of applications: to any atom or ion in any symmetry from spherical to C_1 for any energy interval from the infrared to the x-ray spectral regions; (3) the possibility to take into account all effects of a chemical bond formation such as covalency, ionicity, and configuration interactions; (4) the potential to calculate a wide variety of physical properties (like transition probabilities, for example) using the obtained wave functions of the corresponding energy levels. All relativistic effects, such as spin-orbit interaction and dependence of mass on velocity, are no longer considered as small perturbations, but are taken into account from the very first step of the calculations.

The key idea of the method is that the molecular orbitals (MO) consisting of the wave functions of an impurity ion and ligands are used throughout the calculations rather than atomic wave functions. This makes the effects of the covalent bond formation in a cluster to be taken into account explicitly, since the percentage contribution of wave functions of different ions to any MO can be readily evaluated.

The relativistic many-electron Hamiltonian is expressed as follows (in atomic units $m=e=\hbar=1$):

$$H=\sum_{i=1}^{n}\left[c\boldsymbol{\alpha}\mathbf{p}_i+\beta c^2-\sum_{\nu}\frac{Z_\nu}{|\mathbf{r}_i-\mathbf{R}_\nu|}+V_0(\mathbf{r}_i)+\sum_{\mu}\frac{Z_\mu^{eff}}{|\mathbf{r}_i-\mathbf{R}_\mu|}\right]+\sum_{i=1}^{n}\sum_{j>i}^{n}\frac{1}{|\mathbf{r}_i-\mathbf{r}_j|}, \quad (1)$$

where $\boldsymbol{\alpha}$, β are the Dirac matrices, c the velocity of light, $\mathbf{r}_i$, $\mathbf{p}_i$ the position and the momentum operator of the ith electron, Z_ν and $\mathbf{R}_\nu$ the electrical charge and position of the υth nucleus, Z_μ^{eff} and $\mathbf{R}_\mu$ the electrical charge and position of the μth ion outside the model cluster (in the simplest case, the model cluster consists of the central ion and the host lattice ions of the first coordination sphere. In principle, using clusters with ions from further coordination spheres is also possible, though more computational efforts are needed in this case), n the number of explicitly treated electrons (in our case, $3d$-electrons of Cr^{3+}). In fact, "explicitly treated electrons" are those involved in the considered electron transitions. Since in the present work the main attention is focused on the splitting of $3d$ orbitals of the Cr^{3+} ion, it is natural to consider "explicitly" three d electrons of Cr^{3+}. In case of $L_{2,3}$ x-ray absorption near-edge structure (XANES) spectra, for example, $2p$ and $3d$ electrons are referred to as explicitly treated electrons.[31] $V_0(\mathbf{r}_i)$ is the potential from the remaining electrons (Ref. 33)

$$V_0=\int\frac{\rho_0^G(\mathbf{r}')}{|\mathbf{r}-\mathbf{r}'|}d\mathbf{r}'+\frac{3}{4}\left[\frac{\rho_0^G(\mathbf{r})V_{xc}\{\rho_0^G(\mathbf{r})\}-\rho_0^G(\mathbf{r})V_{xc}\{\rho_0^G(\mathbf{r})\}}{\rho_1^G(\mathbf{r})}-V_{xc}\{\rho_1^G(\mathbf{r})\}\right], \quad (2)$$

where ρ^G, ρ_1^G, ρ_0^G represent the charge density of all electrons, that of the explicitly treated electrons and that of the remaining electrons, respectively; $\rho^G=\rho_1^G+\rho_0^G$ and V_{xc} is the Slater's X_α potential. The superscript G indicates the values for the ground state. Coulomb and exchange interactions between explicitly considered electrons are accounted for by the last term of Eq. (1), whereas all interactions between these n electrons and those of the central ion and ligands are described by Eq. (2). Diagonalization of the Hamiltonian (1) in the basis spanned by all possible Slater determinants for the considered electron configurations gives a complete electron energy level scheme for the considered cluster. The Slater determinants are constructed from the relativistic four-component MO's, which, in turn, can be calculated self-consistently on the basis of the Dirac-Fock-Slater formalism using the relativistic SCAT computation code.[32] Since the eigenfunctions of the corresponding energy levels are also obtained, the absorption spectra (for electric dipole, electric quadrupole, and magnetic dipole transitions) can be obtained in a straightforward manner after calculating the appropriate matrix elements. For example, in the case of electric dipole transitions the oscillator strength (averaged over all possible polarizations) is calculated as follows:

$$I_{if}=\frac{2}{3}(E_f-E_i)\left|\left\langle\Psi_f\left|\sum_{k=1}^{n}\mathbf{r}_\mathbf{k}\right|\Psi_i\right\rangle\right|^2, \quad (3)$$

where Ψ_i and Ψ_f are the initial and final states with energies of E_i and E_f, respectively.

Relativistic effects explicitly considered in this computational method are, of course, more important when heavy elements (such as lanthanides and actinides) or x-ray absorption near-edge structure (XANES) spectra are dealt with (as in Ref. 31). Nevertheless, we use the DVME method in this paper for the analysis of crystal field effects on Cr^{3+} electrons to demonstrate and emphasize the flexibility of this unified approach and its validity for any elements in the Periodic Table.

The method recently has been successfully applied to the analysis of the $4f$-$5d$ absorption spectra of various trivalent lanthanides in $LiYF_4$ (Refs. 34 and 35), high lying $4f$ and $5d$ states of free trivalent lanthanides,[36,37] calculations of the XANES spectra of transition metal ions,[38–41] comparative study of the Cr^{3+} absorption spectra in $ZnAl_2S_4$ and $ZnGa_2O_4$ crystals,[42] and the covalence effects for Cr^{3+}, Mn^{4+}, Fe^{5+} ions in the $SrTiO_3$ crystal.[43] The first application of this method to the microscopic consideration of spectroscopic and dynamic characteristics of impurity centers reported in the present paper enlarges its area of applicability.

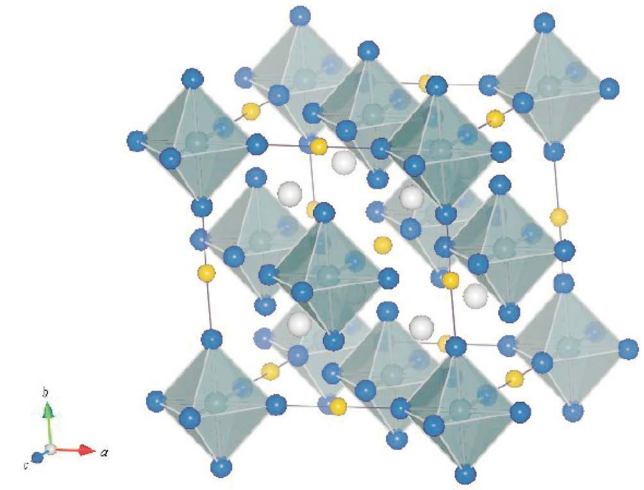

(a)

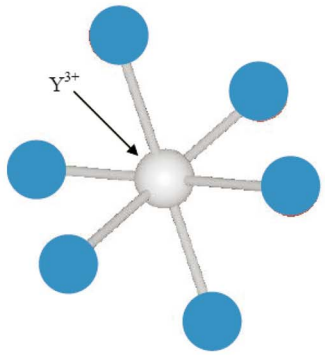

(b)

FIG. 1. (Color online) Crystal structure of Cs_2NaYBr_6. (a) One unit cell. Y^{3+} ions are at the centers of the octahedrons formed by Br^- ions, Na^+ ions are located at the edges of the unit cell between bromine octahedra, Cs^+ ions are located inside the unit cell. (b) Six Br^- ions forming octahedral coordination of Y^{3+} ion (or Cr^{3+} after substitution). Drawn with VENUS developed by Dilanian and Izumi.

III. CRYSTAL STRUCTURE AND SPECTROSCOPY OF Cs_2NaYX_6 (X=F, Cl, Br) CRYSTALS

All considered crystals have the same structure and belong to the cubic $Fm3m$ space group (Fig. 1). One unit cell contains four formula units. Lattice constants are (in Å): 9.075 for Cs_2NaYF_6 (Ref. 44), 10.7396 and 11.3047 for Cs_2NaYCl_6 and Cs_2NaYBr_6, respectively.[45] Increase of the lattice constants is directly related to the increase of the halogen ion radii (1.33 Å for F^-, 1.81 Å for Cl^-, and 1.96 Å for Br^-).[46] Cr^{3+} ion substitutes for the Y^{3+} ion in all these hosts and is surrounded by six halogen ions; since electrical charges of both substituting and substituted ions are equal, no charge compensating additions are required to maintain electric neutrality. However, there is a considerable difference in ionic radii of substituting and substituted ions (0.61 Åfor Cr^{3+} and 0.90 Å for Y^{3+}).[46] Such a difference leads to a significant inward relaxation of the halogen octahedrons around the Cr^{3+} ion and a decrease of the interionic separation. Quantitatively this relaxation can be accounted for by multiplying the $Y^{3+}-F^-$ (Cl^-, Br^-) distance by the ratio $(r_{Cr^{3+}}+r_{halogen})/(r_{Y^{3+}}+r_{halogen})$. With the above given ionic radii this ratio equals 0.87, 0.89, and 0.90 for Cs_2NaYF_6, Cs_2NaYCl_6, and Cs_2NaYBr_6, respectively.

Absorption and luminescence spectra of Cr^{3+} ion in these hosts are typical for the octahedral Cr^{3+} ion and were reported and analyzed previously.[18–30] We will not repeat these data here, but will refer to some of them when discussing the results of our calculations.

IV. THEORETICAL BASIS

Dependence of $10Dq$ on the "impurity ion—ligand" chemical bond length R in the vicinity of the equilibrium position can be represented by the expression (Refs. 6, 7, 9, and 13),

$$10Dq = \frac{K}{R^n}, \tag{4}$$

where K is a constant. The $10Dq(R)$ functional dependence is not only important for the impurity ion energy levels splitting, but influences the EVI between the impurity ion and lattice normal modes.[6] The EVI Hamiltonian in the ${}^4T_{2g}$ state of a $3d^3$ ion (like V^{2+}, Cr^{3+}, Mn^{4+}, Fe^{5+}) in the harmonic approximation (if only a_{1g} and e_g normal modes are considered) can be written in matrix form as follows (Ref. 47):

$$H_{EVI} = V_A \begin{pmatrix} Q_{a_{1g}} & 0 & 0 \\ 0 & Q_{a_{1g}} & 0 \\ 0 & 0 & Q_{a_{1g}} \end{pmatrix} + V_E \begin{pmatrix} \frac{1}{2}Q_{e_{g\theta}} - \frac{\sqrt{3}}{2}Q_{e_{g\varepsilon}} & 0 & 0 \\ 0 & \frac{1}{2}Q_{e_{g\theta}} + \frac{\sqrt{3}}{2}Q_{e_{g\varepsilon}} & 0 \\ 0 & 0 & -Q_{e_{g\theta}} \end{pmatrix}, \tag{5}$$

where V_A, V_E are the constants of the EVI with a_{1g} and e_g normal modes, respectively, and $Q_\theta \sim 3z^2-r^2$ and $Q_\varepsilon \sim x^2-y^2$ are the normal coordinates of the e_g Jahn-Teller active mode. V_A can be expressed in a way similar to $10Dq$ (Ref. 6):

$$V_A = -\frac{nK}{\sqrt{6}R^{n+1}}. \tag{6}$$

Finally, V_E is related to V_A by means of the following simple relation (Ref. 48):

$$V_E = \frac{V_A}{\sqrt{2}}. \tag{7}$$

One of the experimentally observed manifestations of EVI is the energetic Stokes shift $E_S(i)$ (the difference between the maxima of the lowest absorption and emission bands). Due

TABLE I. Values (in cm^{-1}) of $10Dq$ and lowest "ligand-metal" CT transition energy in the $[CrX_6]^{3-}$ cluster embedded into Cs_2NaYX_6 (X=F, Cl, Br) crystals calculated for different values of the Cr^{3+}—halogen distance. Interionic distance is given in units of the Y^{3+}—halogen equilibrium distance r_e, which is 2.268 75 Å for Cs_2NaYF_6 (Ref. 44), 2.619 39 Å for Cs_2NaYCl_6, and 2.765 13 Å for Cs_2NaYBr_6 (Ref. 45). In all approximating functions R is measured in Å, and the calculated result is the energy measured in cm^{-1}.

Cr—Halogen distance	0.825 r_e	0.850 r_e	0.875 r_e	0.900 r_e	0.925 r_e	0.950 r_e	0.975 r_e	1.00 r_e	Approximating functions
					10 Dq				
Cs_2NaYF_6	18007	15704	13771	12141	10762	9590	8587	7564	$\frac{294650}{R^{4.4634}}$
Cs_2NaYCl_6	–	16849	14818	13089	11609	10337	9234	8274	$\frac{557820}{R^{4.3742}}$
Cs_2NaYBr_6	–	16100	14182	12543	11136	9921	8861	7929	$\frac{664190}{R^{4.3532}}$
					CT				
Cs_2NaYF_6	68985	61646	55089	49206	43924	39170	34879	30835	245200−95270R
Cs_2NaYCl_6	–	51291	46418	41908	37719	33827	30210	26853	188710−62071R
Cs_2NaYBr_6	–	45611	40913	37428	33699	30197	26906	23814	167060−51992R

to the ith normal mode, this shift is defined as follows (Refs. 49 and 50):

$$E_S(i) = 2S_i \hbar\, \omega_i = \frac{V_i^2}{M\omega_i^2}, \tag{8}$$

where M is the mass of a single ligand, and S_i stands for the nondimensional Huang-Rhys factor for the ith mode with a frequency ω_i (vibration frequencies can be obtained from Raman spectra or an analysis of the vibronic progressions). For the Cr^{3+} ion in halide crystals the *total* Stokes shift E_S arising from the combined effect of both a_{1g} and e_g modes can be written just as a sum of the individual contributions from each mode (Refs. 49 and 50):

$$E_S = E_S(a_{1g}) + E_S(e_g). \tag{9}$$

This circumstance gives a good opportunity to compare the *calculated* values from Eqs. (8) and (9) Stokes shift with *experimental* values, thus providing a test for the reliability of the calculations.

One additional application of the $10Dq(R)$ function is related to the estimation of the local bulk modulus B around an impurity ion. The following equation holds true (Ref. 10):

$$\left(\frac{\partial 10Dq}{\partial R}\right)_{R=R_0} = -\left(\frac{\partial 10Dq}{\partial P}\right)_{P_0} \frac{3B}{R_0}, \tag{10}$$

where R_0 is the equilibrium position, and the derivative $\frac{\partial 10Dq}{\partial P}$ relates to the pressure dependence of $10Dq$. Having obtained the $10Dq$ dependence, it is also possible to estimate the Grüneisen constant $\gamma(a_{1g})$. It was shown[7] that the Stokes shift for the a_{1g} full-symmetric mode increases with increasing interionic separation:

$$E_S(a_{1g}) = 2S(a_{1g})\, \hbar\, \omega(a_{1g}) \propto R^p, \tag{11}$$

where

$$p = 6\gamma(a_{1g}) - 2(n+1). \tag{12}$$

Then, if the pressure dependence of $S(a_{1g})$ and $\hbar\omega(a_{1g})$ are known, the value of $\gamma(a_{1g})$ can be easily found.

As seen from Eqs. (4)–(12), exact knowledge of the $10Dq(R)$ functional dependence turns out to be an important factor for calculating spectroscopic and elastic constants of crystals.

V. RESULTS OF CALCULATIONS AND DISCUSSION

To analyze the microscopic behavior of Cr^{3+} ion in the chosen hosts, the octahedral $[CrX_6]^{3-}$ (X=F, Cl, Br) cluster, which is formed by the nearest ligands around the Cr^{3+} ion, was used in the calculations. This cluster was embedded into an effective Madelung potential created by several thousand point charges (with formal charges "+1" for Cs, "+1" for Na, "+3" for Y, and "−1" for halogen ions) located at atomic sites outside the cluster. The atomic orbitals used for the calculations were from $1s$ to $4p$ for the Cr^{3+} ion and from $1s$ to $2p$ for F^- ($3p$ for Cl^-, $4p$ for Br^-). Such a cluster is typical for an octahedral Cr^{3+} ion, and inclusion of the Madelung potential for real crystals into the calculations made the final results realistic and reliable.

Table I shows the results of the calculation of the $10Dq$ value (calculated as the energy difference between the Cr^{3+} antibonding e_g and t_{2g} orbitals) in all considered crystals for different distances between the Cr^{3+} ion and the halogen ions. In addition to the crystal field strength, the energies of the lowest CT transitions which correspond to the excitation of the electron from the highest occupied p orbital of ligand to the lowest unoccupied e_g orbital of the Cr^{3+} ion are shown as well (this transition would lead to the highest spin S=2 of a Cr^{2+} ion with a $3d^4$-electron configuration and, in accordance with Hund's rule, to the lowest energy). An increase of the interionic separation is accompanied by a decrease of the $10Dq$ value and CT energy. This trend was reported earlier[9]

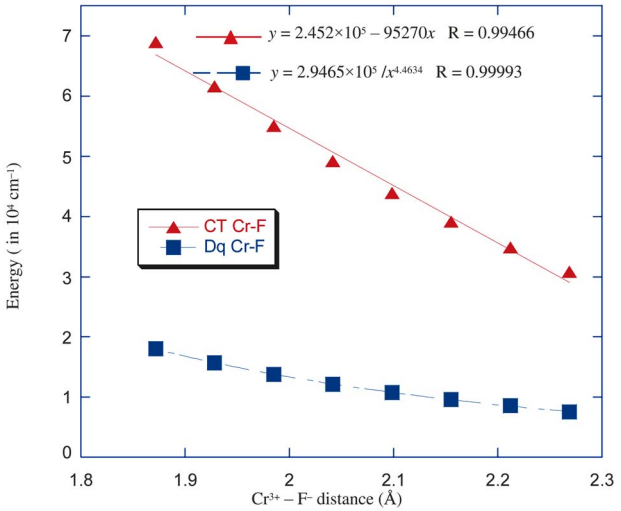

FIG. 2. (Color online) Dependence of $10Dq$ (squares) and CT energy (triangles) on the Cr^{3+}–F^{-} distance in $Cs_2NaYF_6:Cr^{3+}$.

and is confirmed in our calculations as well. The obtained data sets were approximated by linear functions for the CT energies and power laws for the $10Dq$ values; these functions are shown in Table I. Figures 2–4 illustrate the behavior of the CT energy and $10Dq$ as the functions of the interionic separation. It is seen that all calculated values (shown by triangles for the CT energy and squares for $10Dq$) excellently follow the fitting lines. The quality of fitting is shown in each figure by the correlation coefficient R[51] which is practically equal to unity for all lines. In all cases the value of n is about 4.4, in excellent agreement with an earlier reported result,[9] where n was found to be about 3 for the $[CrO_4]^{4-}$ complex and it was stressed that this value for octahedral complexes like $[CrF_6]^{3-}$ would be about 50% higher.

It is possible to relate the results of the lowest CT energy calculations to the values of n. If the ligand's electron is

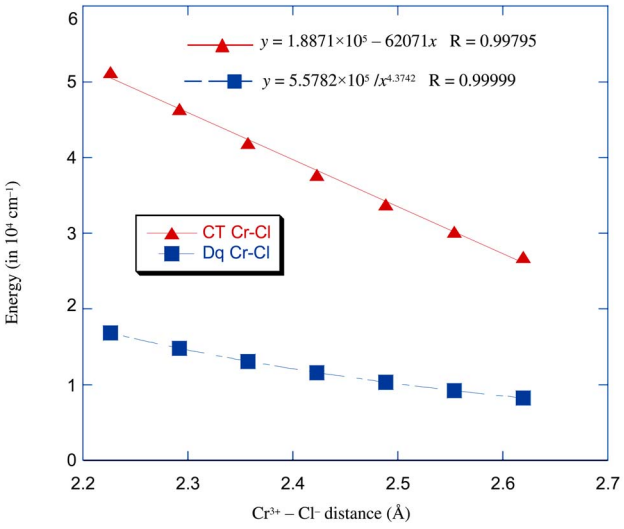

FIG. 3. (Color online) Dependence of $10Dq$ (squares) and CT energy (triangles) on the Cr^{3+}–Cl^{-} distance in $Cs_2NaYCl_6:Cr^{3+}$.

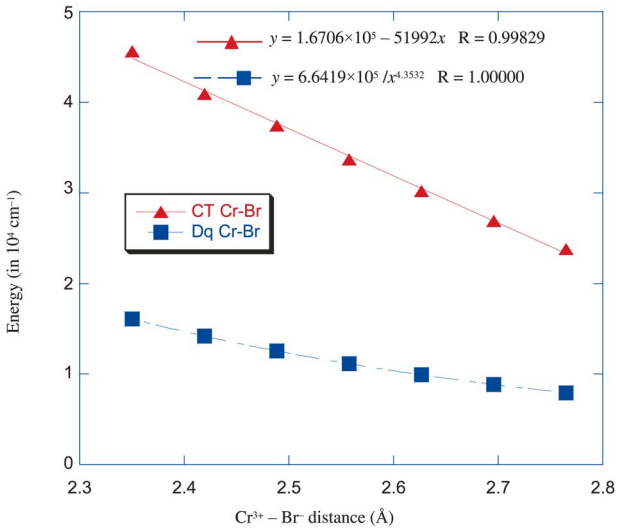

FIG. 4. (Color online) Dependence of $10Dq$ (squares) and CT energy (triangles) on the Cr^{3+}–Br^{-} distance in $Cs_2NaYBr_6:Cr^{3+}$.

excited to the e_g orbital of an impurity ion (situated $10Dq$ above the t_{2g} orbital), the CT transition energy E(CT) in the first approximation is proportional to $10Dq$. Hence the derivative $dE(\mathrm{CT})/dR$ should be proportional to n, being a decreasing function of n. This conclusion is supported by Fig. 5, which indeed shows the linear dependence of $dE(\mathrm{CT})/dR$ on n for all considered crystals. It should not be, however, understood, that such dependence should *always* be linear with the same slope as in Fig. 5. $dE(\mathrm{CT})/dR$ is expected to be a linear function for the octahedrally coordinated ions with three or more d electrons, when CT leads to the formation of a high spin state (for ions with less than three d electrons the lowest CT transition would promote the ligand's p electron into one of the vacant t_{2g}-orbitals, and CT

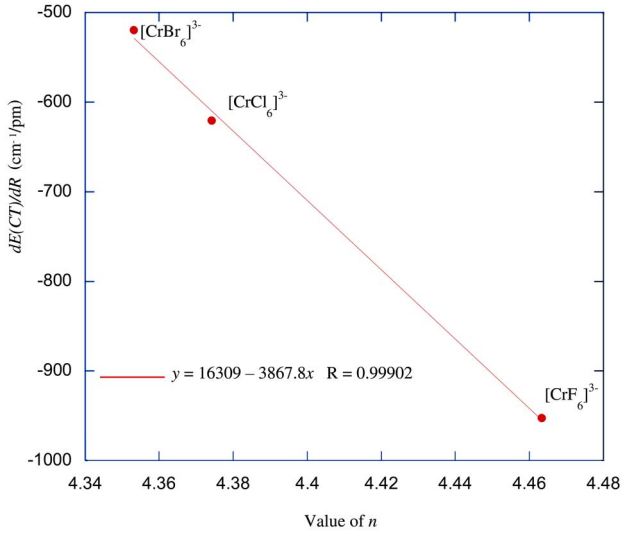

FIG. 5. (Color online) Relation between $dE(\mathrm{CT})/dR$ and n for $Cs_2NaYX_6:Cr^{3+}$ (X=F, Cl, Br). The filled circles are the values of $dE(\mathrm{CT})/dR$ for the corresponding values of n and the straight line is the linear approximation (its equation is given in the figure).

TABLE II. Partial contribution (in %) of the ligands p and s orbitals into $3d$ MO in $Cs_2NaYX_6:Cr^{3+}$ (X=F, Cl, Br) crystals. Values of distance are the same as in Table I.

	Cr–Halogen distance	0.850 r_e	0.875 r_e	0.900 r_e	0.925 r_e	0.950 r_e	0.975 r_e	1.00 r_e
				Cs_2NaYF_6				
t_{2g} states	Cr^{3+} 3d	92.79	92.95	93.05	93.12	93.14	93.12	93.05
	F^- 2p	7.12	7.05	6.95	6.88	6.86	6.88	6.95
	F^-2s	–	–	–	–	–	–	–
e_g states	Cr^{3+} 3d	83.59	83.59	83.52	83.87	83.67	82.91	82.61
	F^-2p	15.69	15.84	16.02	16.27	16.55	16.87	17.21
	F^-2s	0.72	0.57	0.46	0.36	0.28	0.22	0.18
				Cs_2NaYCl_6				
t_{2g} states	Cr^{3+} 3d	92.43	92.70	92.90	93.05	93.15	93.19	93.16
	Cl^-3p	7.56	7.30	7.10	6.95	6.85	6.81	6.84
	Cl^-3s	–	–	–	–	–	–	–
e_g states	Cr^{3+} 3d	77.65	78.07	78.36	78.52	78.56	78.55	78.44
	Cl^-3p	20.76	20.61	20.55	20.58	20.68	20.84	21.06
	Cl^-3s	1.59	1.32	1.09	0.90	0.74	0.61	0.50
				Cs_2NaYBr_6				
t_{2g} states	Cr^{3+} 3d	92.60	92.86	93.06	93.22	93.32	93.36	93.33
	Br^-4p	7.40	7.14	6.94	6.78	6.68	6.64	6.67
	Br^-4s	–	–	–	–	–	–	–
e_g states	Cr^{3+} 3d	75.82	76.29	76.62	76.82	76.89	76.87	76.76
	Br^-4p	22.66	22.46	22.35	22.34	22.42	22.57	22.78
	Br^-4s	1.52	1.25	1.03	0.84	0.69	0.56	0.46

in the first approximation does not depend on $10Dq$). Since the coefficients of the dependence of $dE(\mathrm{CT})/dR$ on n depend in fact on a complicated interrelation between many factors (nature of ligands and impurity ion, effects of chemical pressure,[13] etc.), in principle, they may vary from system to system.

It is also instructive to compare the composition of the $3d$ MO (determined by the Mulliken's population analysis[52]) for the studied compounds (Table II). Though the contribution coming from the Cr^{3+} $3d$ orbitals is, of course, dominating, in all cases there exists a considerable component of the p and small component of the s orbitals from ligand in the $3d$ MO. The latter contribute only to the e_g orbitals, since admixture of the ligand's s states into the metal t_{2g} orbital is forbidden by symmetry.[6] Ligand's contributions increase with increasing the halogen atomic number; therefore, Cs_2NaYBr_6 is the most "covalent" crystal among three hosts studied in the present paper. Also ligand's contribution increase with the decreasing metal-ligand distance. Data from Table II can be directly related to the results of the CT energy calculations from Table I. Increasing ligands' contribution to the $3d$ MO can be explained by decreasing the energy gap between the p orbitals of ligands and $3d$ orbitals of Cr^{3+},and, therefore, increasing the mixture of the Cr^{3+} and ligand's wave functions. Therefore, CT energies should decrease in the following order: $[CrF_6]^{3-} \rightarrow [CrCl_6]^{3-} \rightarrow [CrBr_6]^{3-}$, in agreement with the results shown in Table I.

Table III shows the results of calculations of the EVI constants, Stokes shifts, and Huang-Rhys parameters performed using obtained analytical expressions for $10Dq$. Required frequencies of the a_{1g} and e_g normal modes were taken from literature (corresponding references are given in Table III). Inspection of Table III shows that there is reasonable agreement between the calculated and experimentally obtained Huang-Rhys parameters (apart from Cs_2NaYF_6 crystal), and very good agreement between the calculated and estimated from experimental results Stokes shifts.

Estimations of the lowest CT energy in $Cs_2NaYF_6:Cr^{3+}$ at R_0=1.88 Å yield the value 66 092 cm^{-1}=8.19 eV, which is reasonably close to the one (7.91 eV) reported in Ref. 53 for the $[CrF_6]^{3-}$ unit in K_3CrF_6 (the chosen value R_0=1.88 Å was shown in Ref. 53 to correspond to the minimum of the $^4A_{2g}$ ground state potential surface for the $[CrF_6]^{3-}$ unit).

The lowest CT transitions for the $[CrCl_6]^{3-}$ unit in $Cs_2NaScCl_6$ was measured above 30 000 cm^{-1} by Wenger and Güdel,[54] with the Cr^{3+}–Cl^- distance 2.49 Å. Using this value of R and CT energy approximation for $Cs_2NaYCl_6:Cr^{3+}$ (Table I), the value of 34 153 cm^{-1} can be obtained, which is quite reasonable.

Pressure dependence of the Huang-Phys parameter and normal vibration frequencies can be used to find the value of the Gruneisen constant $\gamma(a_{1g})$ for the fully symmetric mode. As shown in Ref. 7, the Huang-Rhys factor $S(a_{1g})$ increases when R increases [or, in other words, $S(a_{1g})$ decreases when applied pressure increases]. This is possible if the value of p from Eq. (11) is positive. So, the lowest estimation of $\gamma(a_{1g})$ can be obtained in a straightforward manner by solving the inequality $p>0$ (provided the value of n is known). Using

TABLE III. Calculated (this work) values of the EVI constants, Huang-Rhys parameters, and total Stokes shifts for Cr^{3+} in Cs_2NaYF_6, Cs_2NaYCl_6, and Cs_2NaYBr_6 at given Cr^{3+}—halogen distance R_0. E_S was calculated using Eq. (9). Experimental values and vibration frequencies were taken from Ref. 29 for $Cs_2NaYF_6:Cr^{3+}$, from Ref. 56 for $Cs_2NaYCl_6:Cr^{3+}$, and from Refs. 11 and 56 for $Cs_2NaYBr_6:Cr^{3+}$.

	Distance R_0, Å	ω_A, cm^{-1}	ω_E, cm^{-1}	Calculation					Exp.		
				V_A, N[a]	V_E, N[a]	S_A	S_E	E_S, cm^{-1}	S_A	S_E	E_S, cm^{-1}
Cs_2NaYF_6	1.88	501	402	-3.39×10^{-9} (−171)	-2.40×10^{-9} (−121)	2.05	1.99	3654	3.2	0.64	3721
Cs_2NaYCl_6	2.40	298	240	-1.79×10^{-9} (−90)	-1.27×10^{-9} (−64)	1.57	1.65	1663	1.6	1.5	1612
Cs_2NaYBr_6	2.44	183	144	-1.98×10^{-9} (−100)	-1.40×10^{-9} (−70)	3.41	3.50	2256	3.7[b]	3.0[b]	2218

[a]The value in cm^{-1}/pm is given in parenthesis.
[b]The values obtained in 11 from experimental Stokes shifts assuming $S_{tot}=S_A+S_E$ [compare with Eq. (9)].

the values of n from Table I, the lowest estimations of $\gamma(a_{1g})$ are: 1.82 for the $[CrF_6]^{3-}$ complex, 1.79 for the $[CrCl_6]^{3-}$ complex, and 1.78 for the $[CrBr_6]^{3-}$ complex. Decrease in the values of n in the series $[CrF_6]^{3-}\rightarrow[CrCl_6]^{3-}\rightarrow[CrBr_6]^{3-}$is accompanied by a decrease in the lowest possible value of $\gamma(a_{1g})$, in accordance with Eq. (12). No experimental measurements of the pressure effects in Cr^{3+}-doped bromides were reported to our knowledge, that is why we cannot make any further conclusions regarding the $[CrBr_6]^{3-}$ unit and hence leave the obtained result as is. On the contrary, corresponding experimental data for the $[CrF_6]^{3-}$ complex in K_2NaGaF_6 (Ref. 55) and $[CrCl_6]^{3-}$ complex in $Cs_2NaScCl_6$ (Ref. 12) are readily available. Our estimation of the value of $\gamma(a_{1g})$ for the $[CrF_6]^{3-}$ unit agrees well with the Gruneisen constant (1.83) for the a_{1g} mode of the $[CrF_6]^{3-}$ complex in K_2NaGaF_6 reported in Ref. 55. Wenger *et al.*[12]reported detailed measurements of the Huang-Rhys parameter and normal vibrations frequencies as a function of pressure for the $[CrCl_6]^{3-}$ unit. Analysis of their data leads to the value of p in Eq. (11) equal to 12.449 for the a_{1g} mode, and, as a result of the application of Eq. (12), to the value $\gamma(a_{1g})=3.87$ for the $[CrCl_6]^{3-}$ complex.

Finally, the last application considered in the present paper of the obtained $10Dq$ dependence for Cr^{3+} in Cs_2NaYCl_6 is connected with estimation of the compressibility around Cr^{3+} impurity. The application of Eq. (10) implies the knowledge of the pressure dependence of $10Dq$. Wenger *et al.*[12] studied the effects of pressure on the Jahn-Teller effect in $Cs_2NaScCl_6:Cr^{3+}$. From their data on pressure dependence of the $^4T_{2g}$-$^4A_{2g}$ zero-phonon line emission energy in the $[CrCl_6]^{3-}$ unit we estimated $\left(\frac{\partial 10Dq}{\partial P}\right)_{P_0}=17.457$ cm^{-1}/kbar. With the $10Dq$ dependence from Table I and equilibrium distance $R_0=2.40$ Å we found the local bulk modulus $B=101.2$ GPa$=1012$ kbar, and compressibility for the $[CrCl_6]^{3-}$ unit in Cs_2NaYCl_6 $\chi=1/B=9.88\times10^{-4}$ $kbar^{-1}$. The obtained value is close to those reported in Ref. 12 for the $[CrCl_6]^{3-}$ unit in $Cs_2NaScCl_6$ (9.7×10^{-4} $kbar^{-1}$ at 15 K and 1.47×10^{-3} $kbar^{-1}$ at room temperature). We note here that in all our calculations the temperature was set at 0 K.

It is instructive to summarize all of the obtained results and consider how they are affected by the nature of ligands. It is well known that in the $[CrF_6]^{3-}\rightarrow[CrCl_6]^{3-}\rightarrow[CrBr_6]^{3-}$ series the values of $10Dq$, force constants and normal vibrations frequencies are decreasing.[57] Being based on the results of our calculations, we can extend this observation by stating that the values of n in the $10Dq(R)$ dependence and the absolute values of the derivatives $dE(\mathrm{CT})/dR$ for the lowest CT energies follow the same trend. On the contrary, the degree of covalency (related to the ligands contribution to the $3d$ MO) increases when passing from $[CrF_6]^{3-}$ to $[CrBr_6]^{3-}$.

VI. CONCLUSION

As a result of systematic *ab initio* microscopic analysis, the functional dependencies of $10Dq$ and the lowest CT energy on the chemical bond length were obtained for the $[CrX_6]^{3-}$ units in Cs_2NaYX_6 (X=F, Cl, Br) crystals. No empirical or fitting parameters were used in the calculations. Since all calculations are entirely based on the MO concept, not only the Coulomb interaction (which itself is not sufficient to reproduce properly experimental results), but covalent effects and configuration interaction have been taken into account. A simple point charge approximation describes the dependence of $10Dq$ on distance as $1/R^5$, whereas a more elaborate approach developed in the present study shows that $10Dq$ depends on the interionic separation R as $1/R^n$, with $n=4.4634$, 4.3742, and 4.3532 for $Cs_2NaYF_6:Cr^{3+}$, $Cs_2NaYCl_6:Cr^{3+}$, and $Cs_2NaYBr_6:Cr^{3+}$, respectively. Dependence of the lowest CT energy on R is linear for all considered crystals; CT energy decreases when R increases with $dE(\mathrm{CT})/dR=-953$ cm^{-1}/pm, -621 cm^{-1}/pm, and -520 cm^{-1}/pm for $Cs_2NaYF_6:Cr^{3+}$, $Cs_2NaYCl_6:Cr^{3+}$, and $Cs_2NaYBr_6:Cr^{3+}$, respectively. These values can be used for estimations of the lowest CT energies in the $[CrX_6]3^-$ units (X=F, Cl, Br) in other hosts. It was shown that the $dE(\mathrm{CT})/dR$ values for the considered systems depend linearly on the above-given values of n. The $10Dq$ and $E(\mathrm{CT})$ functions obtained as a result of our calculations were used for estimations of the EVI constants, Huang-Rhys parameters, Stokes shifts, and Gruneisen constant $\gamma(a_{1g})$ for all above-mentioned crystals and compressibility around the $[CrCl_6]^{3-}$ unit in Cs_2NaYCl_6. Good agreement between the calculated and experimental (when available) values con-

firms the validity of the obtained results, which can be applied to other octahedral IC formed by the Cr^{3+} ion and the halogen ions. As an additional result, a numerical analysis of the MO composition shows that the covalency increases in the following order: $Cs_2NaYF_6:Cr^{3+} \rightarrow Cs_2NaYCl_6:Cr^{3+} \rightarrow Cs_2NaYBr_6:Cr^{3+}$. Increase of the covalency is followed by a decrease of the CT energy.

In general, reliability of the DVME method in its application to the microscopic analysis of the spectroscopic and elastic parameters related to the 3*d*-ions in crystals was demonstrated in this paper. The computational technique can be applied in a straightforward way to IC formed by other 3*d* ions in crystals.

ACKNOWLEDGMENTS

The present work was partially supported by the "Open Research Center" Project for Private Universities: matching fund subsidy from MEXT (Japanese Ministry of Education, Culture, Sports, Science and Technology), 2004-2008. K. Ogasawara was supported by the individual special research subsidy from Kwansei Gakuin University.

*Corresponding author. E-mail address: brik@fukui.kyoto-u.ac.jp and brik@ksc.kwansei.ac.jp

[1] S. Sugano, Y. Tanabe, and H. Kamimura, *Multiplets of Transition-Metal Ions in Crystals* (Academic Press, New York, 1970).
[2] C. J. Ballhausen, *Introduction to Ligand Field Theory* (McGraw-Hill, New York, 1962).
[3] F. A. Cotton, *Chemical Applications of Group Theory* (John Wiley, New York, 1990).
[4] B. S. Tsukerblat, *Group Theory in Chemistry and Spectroscopy* (Academic Press, London, 1994).
[5] J. Ferguson, H. J. Guggenheim, and D. L. Wood, J. Chem. Phys. **54**, 504 (1971).
[6] M. Moreno, J. A. Aramburu, and M. T. Barriuso, Phys. Rev. B **56**, 14423 (1997).
[7] M. Moreno, M. T. Barriuso, and J. A. Aramburu, J. Phys.: Condens. Matter **4**, 9481 (1992).
[8] M. Moreno, M. T. Barriuso, and J. A. Aramburu, Int. J. Quantum Chem. **52**, 829 (1994).
[9] K. Wissing, J. A. Aramburu, M. T. Barriuso, and M. Moreno, Solid State Commun. **108**, 1001 (1998).
[10] D. Hernández, F. Rodriguez, M. Moreno, and H. U. Güdel, Physica B **265**, 186 (1999).
[11] A. Al-Abdalla, Z. Barandiaran, L. Seijo, and R. Lindh, J. Chem. Phys. **108**, 2005 (1998).
[12] O. S. Wenger, R. Valiente, and H. U. Güdel, J. Chem. Phys. **115**, 3819 (2001).
[13] M. Moreno, M. T. Barriuso, J. A. Aramburu, P. García-Fernández, and J. M. García-Lastra, J. Phys.: Condens. Matter **18**, R315 (2006).
[14] M. C. Marco de Lucas, F. Rodríguez, and M. Moreno, Phys. Rev. B **50**, 2760 (1994).
[15] M. T. Barriuso, M. Moreno, and J. A. Aramburu, Phys. Rev. B **65**, 064441 (2002).
[16] L. Seijo and Z. Barandiaran, J. Chem. Phys. **118**, 1921 (2003).
[17] V. Luaña, M. Bermejo, M. Flórez, J. M. Recio, and L. Pueyo, J. Chem. Phys. **90**, 6409 (1989).
[18] C. M. Delucas, F. Rodriguez, J. M. Dance, M. Moreno, and A. Tressaud, J. Lumin. **48-49**, 553 (1991).
[19] U. Sliwczuk, R. H. Bartram, D. R. Gabbe, and B. C. McCollum, J. Phys. Chem. Solids **52**, 357 (1991).
[20] R. S. Sinkovits and R. H. Bartram, J. Phys. Chem. Solids **52**, 1137 (1991).
[21] A. G. Rinzler, J. F. Dolan, L. A. Kappers, D. S. Hamilton, and R. H. Bartram, J. Phys. Chem. Solids **54**, 89 (1993).
[22] L. Seijo and Z. Barandiaran, J. Chem. Phys. **98**, 4041 (1993).
[23] F. Gilardoni, J. Weber, K. Bellafrouh, C. Daul, and H. U. Güdel, J. Chem. Phys. **104**, 7624 (1996).
[24] R. J. M. da Fonseca, A. D. Tavares, P. S. Silva, T. Abritta, and N. M. Khaidukov, Solid State Commun. **110**, 519 (1999).
[25] R. J. M. da Fonseca, L. P. Sosman, A. D. Tavares, and H. N. Bordallo, J. Fluoresc. **10**, 375 (2000).
[26] G. R. Wein, D. S. Hamilton, U. Sliwczuk, A. G. Rinzler, and R. H. Bartram, J. Phys.: Condens. Matter **13**, 2363 (2001).
[27] R. H. Bartram, G. R. Wein, and D. S. Hamilton, J. Phys.: Condens. Matter **13**, 2377 (2001).
[28] H. N. Bordallo, R. W. Henning, L. P. Sosman, R. J. M. da Fonseca, A. D. Tavares, K. M. Hanif, and G. F. Strouse, J. Chem. Phys. **115**, 4300 (2001).
[29] P. A. Tanner, Chem. Phys. Lett. **388**, 488 (2004).
[30] H. Vrielinck, F. Loncke, F. Callens, P. Matthys, and N. M. Khaidukov, Phys. Rev. B **70**, 144111 (2004).
[31] K. Ogasawara, T. Iwata, Y. Koyama, T. Ishii, I. Tanaka, and H. Adachi, Phys. Rev. B **64**, 115413 (2001).
[32] A. Rosén, D. E. Ellis, H. Adachi, and F. W. Averill, J. Chem. Phys. **65**, 3629 (1976).
[33] S. Watanabe and H. Kamimura, Mater. Sci. Eng., B **3**, 313 (1989).
[34] T. Ishii, K. Fujimura, K. Sato, M. G. Brik, and K. Ogasawara, J. Alloys Compd. **374**, 18 (2004).
[35] K. Ogasawara, S. Watanabe, H. Toyoshima, T. Ishii, M. G. Brik, H. Ikeno, and I. Tanaka, J. Solid State Chem. **178**, 412 (2005); Erratum: *ibid.* **178**, 2175 (2005).
[36] K. Ogasawara, S. Watanabe, Y. Sakai, H. Toyoshima, T. Ishii, M. G. Brik, and I. Tanaka, Jpn. J. Appl. Phys., Part 2 **43**, L611 (2004).
[37] K. Ogasawara, S. Watanabe, T. Ishii, and M. G. Brik, Jpn. J. Appl. Phys., Part 1 **44**, 7488 (2005).
[38] K. Ogasawara, T. Miyamae, I. Tanaka, and H. Adachi, Mater. Trans., JIM **43**, 1435 (2002).
[39] H. Ikeno, I. Tanaka, L. Miyamae, T. Mishima, H. Adachi, and K. Ogasawara, Mater. Trans., JIM **45**, 1414 (2004).
[40] H. Ikeno, I. Tanaka, Y. Koyama, T. Mizoguchi, and K. Ogasawara, Phys. Rev. B **72**, 075123 (2005).
[41] M. G. Brik, K. Ogasawara, T. Ishii, H. Ikeno, and I. Tanaka, Rad. Phys. Chem., doi:10.1016/j.radphyschem.2005.07.055 (2006).
[42] M. G. Brik, Eur. Phys. J. B **49**, 269 (2006).
[43] M. G. Brik, J. Phys. Chem. Solids **67**, 856 (2006).
[44] A. Vedrine, J. P. Besse, G. Baud, and M. Capstan, Rev. Chim.

Miner. **7**, 593 (1990).
[45] G. Reber, H. U. Güdel, G. Meyer, T. Schleid, and C. A. Daul, Inorg. Chem. **28**, 3249 (1989).
[46] R. D. Shannon, Acta Crystallogr., Sect. A: Cryst. Phys., Diffr., Theor. Gen. Crystallogr. **32**, 751 (1976).
[47] M. D. Sturge, Solid State Phys. **20**, 91 (1967).
[48] K. Wissing and J. Degen, Mol. Phys. **95**, 51 (1998).
[49] A. M. Woods, R. S. Sinkovits, J. C. Charpie, W. L. Huang, R. H. Bartram, and A. R. Rossi, J. Phys. Chem. Solids **54**, 543 (1993).
[50] M. T. Barriuso, J. A. Aramburu, and M. Moreno, Phys. Status Solidi B **196**, 193 (1994).
[51] J. M. Chambers, W. S. Cleveland, B. Kleiner, and P. A. Tukey, *Graphical Methods for Data Analysis* (Duxbury Press, Boston, 1983).
[52] R. S. Mulliken, J. Chem. Phys. **23**, 1833 (1955).
[53] J. A. Aramburu, M. Moreno, K. Doclo, C. Daul, and M. T. Barriuso, J. Chem. Phys. **110**, 1497 (1999).
[54] O. S. Wenger and H. U. Güdel, J. Chem. Phys. **114**, 5832 (2001).
[55] J. F. Dolan, A. G. Rinzler, L. A. Kappers, and R. H. Bartram, J. Phys. Chem. Solids **53**, 905 (1992).
[56] R. Knochenmuss, C. Reber, M. V. Rajasekharan, and H. U. Güdel, J. Chem. Phys. **85**, 4280 (1986).
[57] C. K. Jorgensen, *Modern Aspects of Ligand Field Theory* (North Holland, Amsterdam, 1971).